Peering Inside the Planet-Hosting Cervantes Star (μ Arae)

Adi Syahwal Ganda Diputra[1], Farahhati Mumtahana[2], Gerhana Puannandra Putri[2], Rhorom Priyatikanto[2], Muhammad Bayu Saputra[3]

[1] Department of Geophysical Engineering, Bandung Institute of Technology, Indonesia
[2] Research Center for Space, National Research and Innovation Agency, Indonesia
[3] Research Center for Computing, National Research and Innovation Agency, Indonesia
adisyahwalgandadiputra@gmail.com

(Submitted on 07.02.2026; Accepted on 06.03.2026)

Abstract. Cervantes (μ Arae) is a G3IV subgiant, located 15.57 ± 0.02 parsecs from the Sun. Cervantes has several physical properties comparable to those of the Sun, although overall its values are larger. Similarities are also observed in its planetary system, which has been studied, with one of the planets confirmed in the habitable zone. This paper aims to investigate the internal stellar structure of Cervantes, building on initial studies of its influence on the planetary system through modeling experiments. Interior structure modeling was performed using the MESA program. The development of MESA was driven by stellar evolution calculations, which underpin various areas of astrophysical research. Static modeling was conducted based on the star's current phase, with an age of 6 Gyr, producing various physical parameters and dividing the star into zones. Ultimately, the analysis provided key physical parameters such as mass, luminosity, pressure, temperature, radius, and age, along with the zonal division of the stellar interior: the nuclear core ($R < 0.28\,R_\odot$), radiative zone ($0.28 < R_\odot < 0.99$), and convective envelope ($0.99 < R_\odot < 1.349$).

Key words: Cervantes, MESA, interior structure, core, radiative and convective.

1 Introduction

One of the well-known planetary systems is the μ Arae system, which consists of a single star, Cervantes (μ Arae, HD 160691, HR 6585, GJ 691), with four planets orbiting it. The first planet, μ Arae b, was identified by [Butler et al., 2001], followed a year later by the second planet, μ Arae c, identified by [Jones et al., 2002] through observing linear trends in radial velocity data obtained using the Anglo-Australian Telescope. μ Arae d was identified as the third planet using the HARPS spectrometer [Santos et al., 2004a, Santos et al., 2004b], observed over eight nights in June 2004, while μ Arae e, the outermost planet in this system, was identified by [Pepe et al., 2007]. Based on the radial velocity measurements spanning over 17 years, the orbital solution for the planetary system was completed by [Goździewski, 2022] in a study that included eccentricity, orbital period, etc. Cervantes is classified as a yellow subgiant star (G3IV), located at a distance of 15.57 ± 0.02 pc from the Sun [Benedict et al., 2022], observed to have a visual magnitude of 5.1 mag and parallax of 65.6 ± 0.8 mas [Vauclair, 2013].

The complex solar system with many planets makes the μ Arae system interesting to study, which is realized through various astronomical and astrophysical research programs in the fields of astrometry and asteroseismology, such as the NASA Exoplanet Research Program, Geneva Planet Search Program, NASA Astrobiology Program, Anglo-Australian Planet Search Program [Butler et al., 2001], NN-EXPLORE Program [Scott et al., 2018], and others. Stars with planetary systems, such as Cervantes, have physical parameters, especially element abundances, that are quite intriguing to examine, such

as the ratio of helium abundance to metallicity [Izotov and Thuan, 2004]. In studies of the internal structure and evolution of stars, physical parameters such as mass, age, and temperature are also important to investigate.

However, characterizing subgiant planet hosts like Cervantes is fundamentally challenged by the difficulty of accurately determining stellar mass in the evolved red giant regime [Malla et al., 2024]. As A- and F-type progenitors ascend the red giant branch, they become difficult to distinguish from less massive G- and K-type counterparts due to converging effective temperatures and luminosities, making robust mass estimates critical for differentiation. Traditional spectroscopic methods and isochrone fitting often suffer from systematic uncertainties; notably, spectroscopic surface gravities are frequently systematically larger than asteroseismic measurements, which can lead to overestimated stellar and planetary masses. This has fueled a mass controversy where the spectroscopic masses of these evolved hosts are suspected of being overestimated by up to 50 per cent compared to kinematic and population-based models [Lloyd, 2011]. Additionally, these stars occupy regions of the Hertzsprung–Russell diagram where evolutionary tracks are tightly packed or overlapping, making it arduous to isolate specific stellar properties without precise, model-independent methods like asteroseismology to resolve discrepancies [Veras, 2016].

Driven by the need to resolve the complexities of post-main-sequence evolution, this research seeks to determine the precise static structure of Cervantes by leveraging the MESA (Modules for Experiments in Stellar Astrophysics) software suite [Paxton et al., 2010]. As a subgiant, Cervantes undergoes rapid internal structural transitions like the contraction of its helium core and the expansion of its outer envelope. Those transitions are difficult to capture through observation alone. By generating a high-fidelity model, we can establish a robust baseline of the star's current physical state, including its interior density profile and chemical gradients. This model serves as a vital foundation for exploring the long-term dynamical evolution of its four known planets, allowing us to predict how burgeoning stellar radii and intensifying tidal interactions will reshape the architecture of the entire planetary system.

2 Physical Characteristics of Cervantes

As explained in the Introduction, the entry point of our research is a literature review to determine and select the physical parameters of the star as input for the MESA program. Observational and measurement-derived physical parameters were prioritised over modelling results [Mumtahana, 2020]. Asteroseismology studies related to spectroscopic observations of Cervantes were conducted by [Soriano and Vauclair, 2010]. Physical parameters of the star, such as age, mass, radius, effective temperature, luminosity, metallicity, etc., were obtained from this study. In addition to [Soriano and Vauclair, 2010], subsequent asteroseismology studies on Cervantes were performed by researchers including [Vauclair, 2013], [Bonfanti et al., 2015], [Soto and Jenkins, 2018], as well as [Mathur et al., 2012]. The following equation is the basic calculation for the Z fraction from metallicity data [Bertelli et al., 1994]. The value of [Fe/H] was chosen by calculating the mean of all [Fe/H] values obtained from

the literature review.

$$\log Z = 0.977\,[\mathrm{Fe/H}] - 1.699 \tag{1}$$

3 Modelling using MESA

MESA has revolutionized the field of stellar modeling by providing an open-source, highly versatile, and 1D computational instrument capable of simulating a star's entire life cycle. Its power lies in its modular architecture, which allows researchers to swap out different physical modules – such as nuclear reaction networks, opacities, and equations of state – to suit specific research goals. This flexibility is paired with robust implicit hydrodynamics, enabling MESA to handle everything from the stable hydrogen-burning of sun-like stars to the violent, rapid transitions of supernova progenitors [Paxton et al., 2018].

In the realm of exoplanet studies, MESA has become an indispensable tool for characterizing the missing half of any planetary system: the host star. Because exoplanet properties like mass and radius are measured relative to their stars, the high-fidelity evolutionary tracks produced using MESA [Dotter, 2016, Choi et al., 2016] are essential for reducing uncertainties. Beyond just the star, MESA's capabilities extend to modeling giant planets themselves, allowing simulation of the internal structure and thermal cooling of gas giants down to one-tenth the mass of Jupiter [Paxton et al., 2013].

The MESA program was developed to solve numerical calculations related to stellar physics. Therefore, several equations must be solved, such as conservation of mass, hydrostatic equilibrium, the equation of state, and energy generation. These numerical calculations produce values for the star's physical parameters, including mass, density, temperature, pressure, luminosity, mass fractions of various elements (H, He, C, N, O, etc.), and energy transport mechanisms as a function of the star's radius [Paxton et al., 2010].

Table 1. Physical parameters of Cervantes [Soriano and Vauclair, 2010]

Parameter	Value
Mass ($M_\odot$)	1.10 ± 0.02
Radius ($R_\odot$)	1.36 ± 0.06
$\log g$ (dex)	4.215 ± 0.005
Effective temperature (K)	5820 ± 50
Luminosity ($L_\odot$)	1.90 ± 0.10
Metallicity [Fe/H]	0.32 ± 0.02
Helium abundance Y	0.30 ± 0.01
Age (Gyr)	6.34 ± 0.80

Physical parameters of Cervantes, derived from asteroseismological analysis via spectroscopic observations by [Soriano and Vauclair, 2010] (see Table 1), were used in this study as the range for initial input conditions. Table 2 shows some physical parameters of the Cervantes star reported in various

Table 2. Physical parameters of Cervantes obtained from various literature sources.

Parameter	Value(s)
Age (Gyr)	6.7^{1}; 5.7 ± 0.6^{3}; 6.34 ± 0.80^{4}; 6.4^{12}
$T_{\rm eff}$ (K)	5773^{2}; 5813 ± 40^{4}; 5770 ± 50^{5}; 5800 ± 100^{6}; 5811 ± 45^{7}; 5798 ± 33^{8}; 5813 ± 40^{9}; 5784 ± 44^{10}; 5807 ± 30^{14}
$\log g$	4.2 ± 0.1^{2}; 4.30 ± 0.10^{6}; 4.42 ± 0.06^{7}; 4.31 ± 0.08^{8}; 4.25 ± 0.07^{9}; 4.30 ± 0.06^{10}
[Fe/H] (dex)	0.28 ± 0.03^{2}; 0.32 ± 0.05^{4}; 0.32 ± 0.05^{5}; 0.32 ± 0.10^{6}; 0.28 ± 0.03^{7}; 0.32 ± 0.04^{8}; 0.32 ± 0.05^{9}; 0.29 ± 0.03^{10}; 0.32^{13}; 0.33 ± 0.03^{14}
Mass ($M_{\odot}$)	1.13 ± 0.02^{3}; 1.10 ± 0.02^{4}; 1.13 ± 0.02^{14}
Radius ($R_{\odot}$)	1.33 ± 0.02^{3}; 1.36 ± 0.06^{4}
$\log(L/L_{\odot})$	0.28 ± 0.012^{5}; 0.28 ± 0.0012^{11}

Notes. Superscripts indicate literature sources: [1] [Goździewski, 2022]; [2] [Soto and Jenkins, 2018]; [3] [Bonfanti et al., 2015]; [4] [Soriano and Vauclair, 2010], [Santos et al., 2004a, Santos et al., 2004b]; [5] [Vauclair, 2013]; [6] [Bensby et al., 2003]; [7] [Laws et al., 2003]; [8] [Santos et al., 2004a]; [9] [Santos et al., 2004b]; [10] [Fischer and Valenti, 2005]; [11] [Bazot et al., 2005]; [12] [Saffe et al., 2005]; [13] [Bouchy et al., 2005]; [14] [Soubiran et al., 2016] and [Ségransan et al., 2010] in [Morgan et al., 2025].

sources in the literature. Subsequently, specific physical parameters were selected as primary input data, including mass and metallicity fraction, and age as the stopping condition (see Table 3) for the modelling process. The range of Cervantes' physical parameters yields various possible modelling scenarios. Therefore, in this study, parameter values were determined by averaging all available values from diverse references to obtain representative estimates. This program operates from the pre-main-sequence phase up to the current condition (subgiant phase).

Table 3. MESA input and stop parameter

Parameter	Value
Mass ($M_{\odot}$)	1.115
Z	0.0401671
Age (Gyr)	6
MLTα	1.8845

In this study, convective overshooting is neglected because its impact on stellar evolution is small, as indicated by [Claret and Torres, 2016, Claret and Torres, 2017, Claret and Torres, 2018, Claret and Torres, 2019], and it only

becomes significant for stars with masses above about $1.2\,M_{\odot}$. In contrast, the choice of the mixing-length parameter in this work is motivated by the presence of a convective envelope in stars with masses between 0.5 and $1.2\,M_{\odot}$ [Joyce and Tayar, 2023], for which value of MLT$\alpha = 1.8845$ is estimated using the linear model of [Viani et al., 2018], which relates the MLTα to the stellar physical parameters (adopted [Soriano and Vauclair, 2010]) by using the solar reference value MLT$\alpha = 1.70098$. The MLTα value used in this study is also close to the one reported by [Henyey et al., 1965].

4 Results and Analysis

The values shown in Table 4 represent all physical parameters of Cervantes resulting from MESA calculations, which are considered sufficiently accurate as they fall within the error ranges of the primary references, [Soriano and Vauclair, 2010]. Referring to the MESA calculation results, curves illustrating the relationships between various physical parameters of Cervantes can be produced. In this study, which aims to reconstruct the interior structure, curves depicting the relationships between physical parameters such as mass, temperature, density, pressure, luminosity, mass fractions, and energy transport mechanisms relative to radius will be generated and discussed.

Table 4. MESA results for Cervantes' physical parameters

Parameter	Value
Mass ($M_{\odot}$)	1.115
Radius ($R_{\odot}$)	1.3699
$\log g$ (dex)	4.2120
Effective temperature (K)	5780.6
Luminosity ($L_{\odot}$)	1.8878
Age (Gyr)	6

4.1 Mass-Density and Pressure-Temperature Relation

In this section, using Fig. 1, the mass, density, temperature, and pressure profiles are presented as functions of radius for the star Cervantes. The mass increases significantly with radius, particularly within the range $0.0 < R_{\odot} < 0.6$, and begins to level off at $R_{\odot} > 0.9$. In contrast, the density exhibits the opposite trend, especially within $0.0 < R_{\odot} < 0.2$, reaching a maximum value of 490 g/cm^3, which is considerably higher than that of the Sun, at only 150 g/cm^3. Consequently, Cervantes is classified as a subgiant star. Fig. 1 also shows that the material near the stellar surface consists of lower-density matter.

Similar to the density profile, both pressure and temperature exhibit the same trends. The maximum pressure reaches 5.78×10^{17} dyne/cm^2, which is

higher than that of the Sun at 2.65×10^{17} dyne/cm^2, and decreases sharply for $R < 0.2R_\odot$. The pressure then declines more gradually within the range $0.2 < R_\odot < 0.3$ and becomes nearly constant for $R > 0.3R_\odot$. Meanwhile, the highest temperature is recorded at 1.865×10^7 K in the stellar core, indicating that the gas is fully ionised in this region. At lower temperatures, ionisation occurs only partially. Compared with the Sun, whose core temperature is approximately 1.5×10^7 K, the temperature of Cervantes is notably higher.

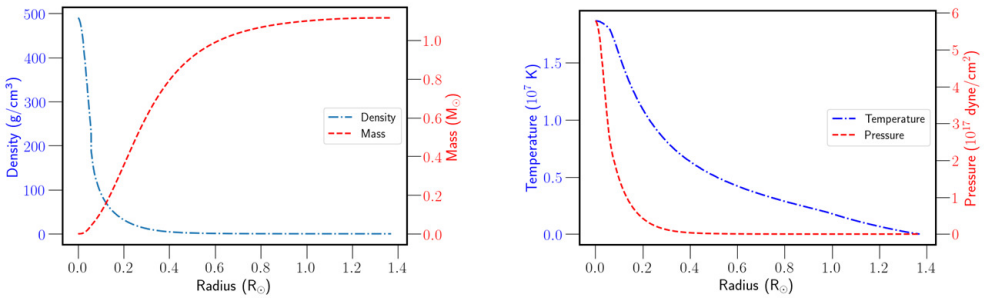

Fig. 1. Mass and density profiles as functions of radius (left), temperature and pressure profiles as functions of radius (right)

4.2 Luminosity and Energy Generation

In this section, Fig. 2 presents the luminosity and energy generation profiles as functions of radius for the Cervantes star. A significant increase in luminosity occurs within the region $R < 0.28R_\odot$, beyond which the luminosity remains approximately constant. The resulting luminosity of Cervantes is also higher than that of the Sun, with a value of $1.98L_\odot$. Fig. 2 additionally displays the energy generation profile ($\mathrm{d}L/\mathrm{d}r$) as a function of radius. From this profile, it is evident that the stellar core is located within the region $R < 0.28R_\odot$.

4.3 Element Abundances

In this section, Fig. 3 presents the abundance profiles of various chemical elements, including hydrogen, helium, carbon, nitrogen, oxygen, and others as functions of radius. The abundance curves, particularly those of hydrogen and helium, indicate the occurrence of nuclear burning in the stellar core, whereby hydrogen is converted into helium. This hydrogen-burning process corresponds to the fusion of four ^{1}H nuclei into a ^{4}He nucleus. The abundance of ^{3}He reaches its maximum value of 0.0026. [Soriano and Vauclair, 2010] reported that the Cervantes (μ Arae) system exhibits an enhanced helium abundance, consistent with the principles of galactic chemical evolution [Izotov and Thuan, 2004]. In the present study, the lower helium abundance compared with that of τ Ceti [Mumtahana, 2020] is attributed to subsequent nuclear fusion processes

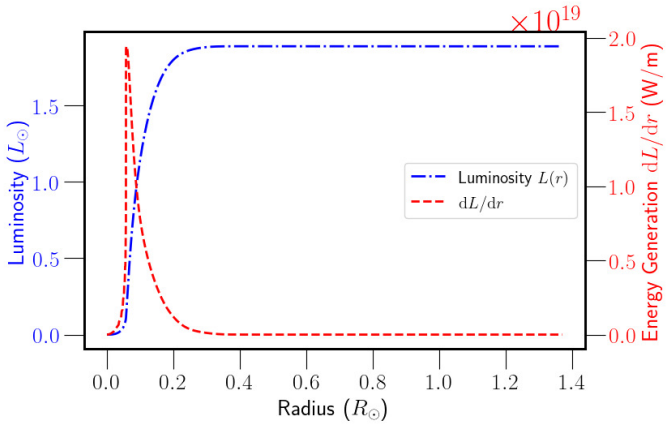

Fig. 2. Luminosity and energy generation profiles as a function of radius

producing carbon and oxygen during the subgiant stage of the Cervantes star (see the right panel of Fig. 3).

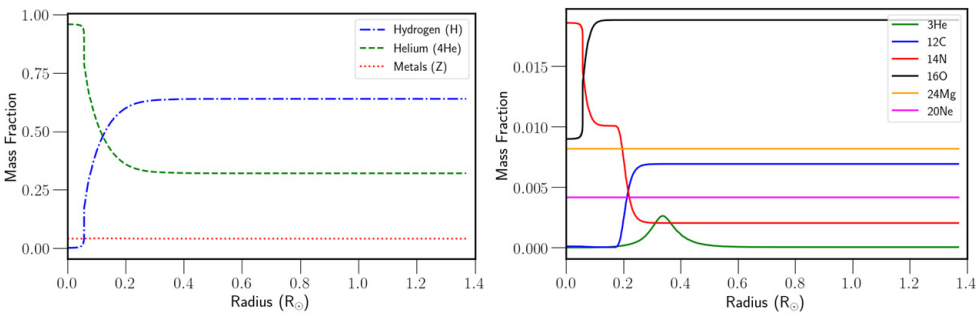

Fig. 3. Mass fractions of the various elements in Cervantes

The high temperature of Cervantes enables the operation of the CNO cycle [Pols, 2011]. As shown in the right panel of Fig. 3, a significant increase in the abundances of ^{12}C occurs at a radius of $0.18 < R_\odot < 0.28$ and ^{16}O reach its peak at a radius of $> 0.11 R_\odot$, whereas the abundances of ^{24}Mg and ^{20}Ne remain constant throughout the stellar radius.

4.4 Energy Transport Mechanism

In the stellar interior, the transport of energy from high temperature regions to lower temperature regions occurs through two mechanisms, namely convection

and radiation. The left panel of Fig. 4 illustrates the energy transport mechanism in Cervantes through the relationship between $d \ln P / d \ln T$ and radius, where efficient energy transport is identified by values exceeding 2.5 [Pols, 2011]. Based on the MESA calculations, radiative energy transport operates in Cervantes up to a radius of $0.99\,R_{\odot}$, while the convective envelope lies above this radius.

The division between the two energy transport zones is further confirmed by the curve of convective velocity as a function of radius (Fig. 4, right panel), where the convective velocity begins to increase at a radius of $0.99\,R_{\odot}$ and rises significantly before returning to zero at the stellar surface. An additional confirmation of the boundary between the radiative zone and the convective envelope is provided by the Schwarzschild stability criterion, represented by the radial profile of $\nabla_{\rm rad} - \nabla_{\rm ad}$. As shown in Fig. 5, this quantity remains negative throughout most of the stellar interior, indicating radiative stability and crosses zero at a radius of approximately $0.99\,R_{\odot}$. Beyond this radius, $\nabla_{\rm rad} - \nabla_{\rm ad}$ becomes positive, signifying the onset of convective instability. This is also consistent with the transition radius inferred from the energy transport mechanism and convective velocity curve.

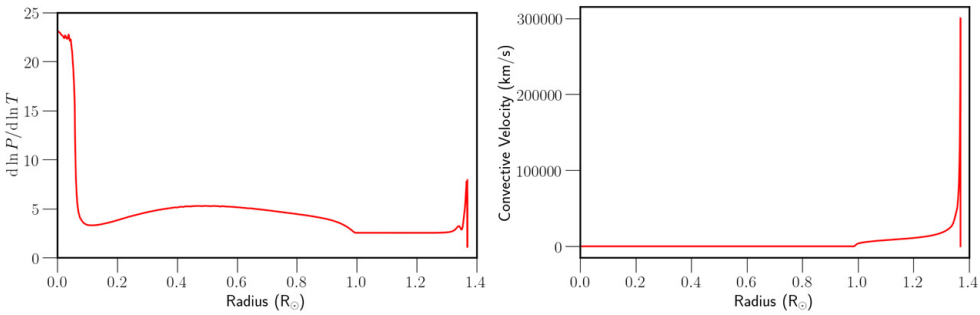

Fig. 4. Energy transport mechanism curves (left) and convective velocity (right) as a function of radius

4.5 Cervantes Interior Structure

In this section, as illustrated in Fig. 6, the interior structure of the star Cervantes is modelled using the radius dependence of the stellar physical parameters discussed previously. The nuclear core of the star extends to a radius of $0.28\,R_{\odot}$, as determined from Figs. 2 and 3. The radiative zone occupies the region $0.28 < R < 0.99\,R_{\odot}$, based on the left panel of Fig. 4, while the convective envelope spans $0.99 < R < 1.349\,R_{\odot}$ according to the right panel of Fig. 4. Consequently, the radiative zone contributes to approximately 52% of the total stellar radius, followed by the convective envelope at 27%, and the nuclear core at around 21%.

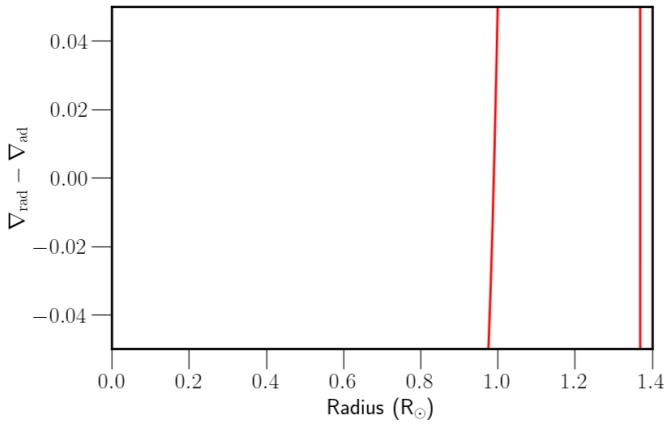

Fig. 5. Schwarzschild stability criterion

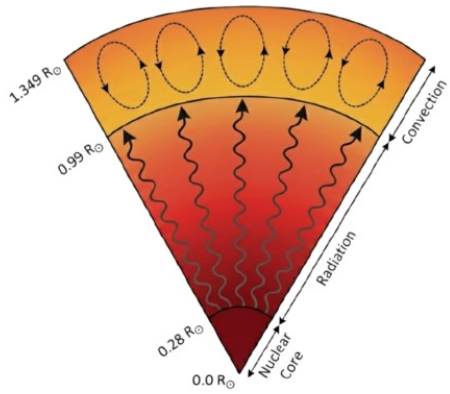

Fig. 6. Schematic of Cervantes interior structure

5 Discussion and Conclusion

The study of stellar interior structure can be carried out through calculations and modelling using the MESA program. In this work, the star Cervantes (μ Arae) was selected as the object of study because it hosts four orbiting planets and is classified as a metal-rich subgiant star. The modelling results indicate that stellar mass and luminosity increase with radius, whereas density, temperature, and pressure decrease outward. Nuclear fusion reactions occurring during the main-sequence phase are dominated by the conversion of hydrogen into helium, followed by subsequent fusion processes that produce heavier elements such as carbon and oxygen. Based on the modelling results, the nuclear core of Cervantes is estimated to extend to a radius of approximately $0.28\,R_\odot$ (Fig. 2 and Fig. 3), while the radiative zone and convective

envelope occupy the regions $0.28 < R < 0.99\,R_{\odot}$ and $0.99 < R < 1.349\,R_{\odot}$, respectively (Fig. 4). Determining the internal stellar structure in this manner provides a useful reference for modelling stellar evolution and for examining the nucleosynthesis and energy transport processes that shape stellar interiors.

In addition to stellar interior properties, the present MESA model offers a starting point for exploring the evolution of the planetary system orbiting Cervantes. The radius and luminosity values obtained from the model (Table 4) suggest that Cervantes has already entered a post–main-sequence phase. As stellar luminosity continues to evolve, the location of the circumstellar habitable zone is expected to change over time, as discussed in theoretical studies of evolving habitable zones [Kasting et al., 1993, Kopparapu et al., 2013, Ramirez and Kaltenegger, 2014]. Consequently, planets currently located within or near the habitable zone of the μ Arae system may experience potentially habitable conditions only during specific evolutionary intervals. Incorporating stellar luminosity–age relations derived from MESA into planetary climate models therefore represents a natural extension of the present work.

As Cervantes evolves further toward the red giant branch, continued stellar expansion and changes in envelope structure are expected to enhance tidal interactions between the star and its close-in planets. Previous studies have shown that such interactions may lead to orbital decay and, in some cases, planetary engulfment [Villaver and Livio, 2009, Villaver et al., 2014, Mustill and Villaver, 2012]. The present interior structure model helps to constrain the current evolutionary stage of Cervantes and provides relevant input parameters, such as stellar radius and envelope structure, that are required for future tidal and engulfment studies. Time-dependent stellar evolution modelling will therefore be necessary to investigate when these processes become significant and how they may affect the long-term stability of the μ Arae planetary system.

In summary, this study presents a static interior model of Cervantes that is consistent with available observational constraints and provides a framework for future investigations. Extending the present MESA modelling to include long-term stellar evolution will allow a more detailed exploration of habitable-zone evolution, planetary orbital decay, and potential engulfment scenarios. Such an approach is expected to improve our understanding of the coupled evolution of stars and their planetary systems, particularly for evolved, planet-hosting stars similar to μ Arae.

Acknowledgements

The authors express their gratitude to Angga Novicensius NB A.Md.T. for providing access to his laptop for computational and modelling purposes.

References

Bazot, M., Vauclair, S., Bouchy, F., and Santos, N. C. (2005). Seismic analysis of the planet-hosting star μ arae. *Astronomy and Astrophysics*, 440(2):615–621.

Benedict, G. F., McArthur, B. E., Nelan, E. P., Wittenmyer, R., Barnes, R., Smotherman, H., and Horner, J. (2022). The μ arae planetary system: Radial velocities and astrometry. *The Astronomical Journal*, 163(6):295.

Bensby, T., Feltzing, S., and Lundström, I. (2003). Elemental abundance trends in the galactic thin and thick disks as traced by nearby f and g dwarf stars. *Astronomy and Astrophysics*, 410(2):527–551.

Bertelli, G., Bressan, A., Chiosi, C., Fagotto, F., and Nasi, E. (1994). Theoretical isochrones from models with new radiative opacities. *Astronomy and Astrophysics Supplement Series*, 106:275.

Bonfanti, A., Ortolani, S., Piotto, G., and Nascimbeni, V. (2015). Revising the ages of planet-hosting stars. *Astronomy and Astrophysics*, 575:A18.

Bouchy, F., Bazot, M., Santos, N. C., Vauclair, S., and Sosnowska, D. (2005). Asteroseismology of the planet-hosting star μ arae. *Astronomy and Astrophysics*, 440(2):609–614.

Butler, R. P., Tinney, C. G., Marcy, G. W., Jones, H. R. A., Penny, A. J., and Apps, K. (2001). Two new planets from the anglo-australian planet search. *The Astrophysical Journal*, 555(1):410–417.

Choi, J., Dotter, A., Conroy, C., Cantiello, M., Paxton, B., and Johnson, B. D. (2016). Mesa Isochrones and Stellar Tracks (MIST). I. Solar-scaled Models. *ApJ*, 823(2):102.

Claret, A. and Torres, G. (2016). The dependence of convective core overshooting on stellar mass. *Astronomy & Astrophysics*, 592:A15.

Claret, A. and Torres, G. (2017). The dependence of convective core overshooting on stellar mass: A semi-empirical determination using the diffusive approach with two different element mixtures. *The Astrophysical Journal*, 849(1):18.

Claret, A. and Torres, G. (2018). The dependence of convective core overshooting on stellar mass: Additional binary systems and improved calibration. *The Astrophysical Journal*, 859(2):100.

Claret, A. and Torres, G. (2019). The dependence of convective core overshooting on stellar mass: Reality check and additional evidence. *The Astrophysical Journal*, 876(2):134.

Dotter, A. (2016). MESA Isochrones and Stellar Tracks (MIST) 0: Methods for the Construction of Stellar Isochrones. *ApJS*, 222(1):8.

Fischer, D. A. and Valenti, J. (2005). The planet-metallicity correlation. *The Astrophysical Journal*, 622(2):1102–1117.

Goździewski, K. (2022). The orbital architecture and stability of the μ arae planetary system. *Monthly Notices of the Royal Astronomical Society*, 516(4):6096–6115.

Henyey, L., Vardya, M. S., and Bodenheimer, P. (1965). Studies in stellar evolution. iii. the calculation of model envelopes. *The Astrophysical Journal*, 142:841.

Izotov, Y. I. and Thuan, T. X. (2004). Systematic effects and a new determination of the primordial abundance of ^{4}he and dy/dz from observations of blue compact galaxies. *The Astrophysical Journal*, 602(1):200–230.

Jones, H. R. A., Butler, R. P., Marcy, G. W., Tinney, C. G., Penny, A. J., McCarthy, C., and Carter, B. D. (2002). Extrasolar planets around hd 196050, hd 216437 and hd 160691. *Monthly Notices of the Royal Astronomical Society*, 337(4):1170–1178.

Joyce, M. and Tayar, J. (2023). A review of the mixing length theory of convection in 1d stellar modeling. *Galaxies*, 11(3):75.

Kasting, J. F., Whitmire, D. P., and Reynolds, R. T. (1993). Habitable zones around main sequence stars. *Icarus*, 101(1):108–128.

Kopparapu, R. K., Ramirez, R., Kasting, J. F., Eymet, V., Robinson, T. D., Mahadevan, S., Terrien, R. C., Domagal-Goldman, S., Meadows, V., and Deshpande, R. (2013). Habitable zones around main-sequence stars: New estimates. *The Astrophysical Journal*, 765(2):131.

Laws, C., Gonzalez, G., Walker, K. M., Tyagi, S., Dodsworth, J., Snider, K., and Suntzeff, N. B. (2003). Parent stars of extrasolar planets. vii. new abundance analyses of 30 systems. *The Astronomical Journal*, 125(5):2664–2677.

Lloyd, J. P. (2011). "Retired" Planet Hosts: Not So Massive, Maybe Just Portly After Lunch. *ApJ*, 739(2):L49.

Malla, S. P., Stello, D., Montet, B. T., Huber, D., Hon, M., Bedding, T. R., Reyes, C., and Hey, D. R. (2024). Benchmarking the spectroscopic masses of 249 evolved stars using asteroseismology with tess. *Monthly Notices of the Royal Astronomical Society*, 534(3):1775–1786.

Mathur, S., Metcalfe, T. S., Woitaszek, M., Bruntt, H., Verner, G. A., Christensen-Dalsgaard, J., and others (2012). A uniform asteroseismic analysis of 22 solar-type stars observed by *Kepler*. *The Astrophysical Journal*, 749(2):152.

Morgan, M., Bowler, B. P., Tran, Q. H., Wittenmyer, R. A., Wright, D. J., Zhou, G., and Fairnington, T. R. (2025). Exploring warm jupiter migration pathways with eccentricities. i. catalog of uniform keplerian fits to radial velocities of 200 warm jupiters.

Mumtahana, F. (2020). Interior structure of solar-like star τ ceti. *Journal of Physics: Conference Series*, 1523(1):012012.

Mustill, A. J. and Villaver, E. (2012). Foretellings of ragnarök: World-engulfing asymptotic giants and the inheritance of white dwarfs. *The Astrophysical Journal*, 761(2):121.

Paxton, B., Bildsten, L., Dotter, A., Herwig, F., Lesaffre, P., and Timmes, F. (2010). Modules for experiments in stellar astrophysics (mesa). *The Astrophysical Journal Supplement Series*, 192(1):3.

Paxton, B., Cantiello, M., Arras, P., Bildsten, L., Brown, E. F., Dotter, A., Mankovich, C., Montgomery, M. H., Stello, D., Timmes, F. X., and Townsend, R. (2013). Modules for Experiments in Stellar Astrophysics (MESA): Planets, Oscillations, Rotation, and Massive Stars. *ApJS*, 208(1):4.

Paxton, B., Schwab, J., Bauer, E. B., Bildsten, L., Blinnikov, S., Duffell, P., Farmer, R., Goldberg, J. A., Marchant, P., Sorokina, E., Thoul, A., Townsend, R. H. D., and Timmes, F. X. (2018). Modules for Experiments in Stellar Astrophysics (MESA): Convective Boundaries, Element Diffusion, and Massive Star Explosions. *ApJS*, 234(2):34.

Pepe, F., Correia, A., Mayor, M., Tamuz, O., Couetdic, J., Benz, W., Bertaux, J.-L., Bouchy, F., Laskar, J., Lovis, C., et al. (2007). The harps search for southern extra-solar planets-viii. μ arae, a system with four planets. *Astronomy & Astrophysics*, 462(2):769–776.

Pols, O. R. (2011). *Stellar Structure and Evolution*. Astronomical Institute Utrecht. Lecture Notes.

Ramirez, R. M. and Kaltenegger, L. (2014). The habitable zones of pre-main-sequence stars. *The Astrophysical Journal Letters*, 797(2):L25.

Saffe, C., Gómez, M., and Chavero, C. (2005). On the ages of exoplanet host stars. *Astronomy and Astrophysics*, 443(2):609–626.

Santos, N. C., Bouchy, F., Mayor, M., Pepe, F., Queloz, D., Udry, S., and Vauclair, S. (2004a). The harps survey for southern extra-solar planets. *Astronomy and Astrophysics*, 426(1):L19–L23.

Santos, N. C., Israelian, G., and Mayor, M. (2004b). Spectroscopic [fe/h] for 98 extra-solar planet-host stars. *Astronomy and Astrophysics*, 415(3):1153–1166.

Scott, N. J., Howell, S. B., Horch, E. P., and Everett, M. E. (2018). The nn-explore exoplanet stellar speckle imager: Instrument description and preliminary results. *Publications of the Astronomical Society of the Pacific*, 130(987):054502.

Ségransan, D., Udry, S., Mayor, M., Naef, D., Pepe, F., Queloz, D., and others (2010). The coralie survey for southern extrasolar planets. *Astronomy and Astrophysics*, 511:A45.

Soriano, M. and Vauclair, S. (2010). New seismic analysis of the exoplanet-host star μ arae. *Astronomy and Astrophysics*, 513:A49.

Soto, M. G. and Jenkins, J. S. (2018). Spectroscopic parameters and atmospheric chemistries of stars (species). *Astronomy and Astrophysics*, 615:A76.

Soubiran, C., Le Campion, J.-F., Brouillet, N., and Chemin, L. (2016). The pastel catalogue: 2016 version. *Astronomy and Astrophysics*, 591:A118.

Vauclair, S. (2013). Seismic studies of planet-harbouring stars. *Proceedings of the International Astronomical Union*, 9(S301):353–358.

Veras, D. (2016). Post-main-sequence planetary system evolution. *Royal Society Open Science*, 3(2):150571.

Viani, L. S., Basu, S., Joel, M., Johnson, J. A., Bonaca, A., and Chaplin, W. J. (2018). Investigating the metallicity–mixing-length relation. *The Astrophysical Journal*, 858(1):28.

Villaver, E. and Livio, M. (2009). The orbital evolution of gas giant planets around giant stars. *The Astrophysical Journal Letters*, 705(1):L81–L85.

Villaver, E., Livio, M., Mustill, A. J., and Siess, L. (2014). Hot jupiters and cool stars. *The Astrophysical Journal*, 794(1):3.